Chapter 4: Design and Simulation Studies of Millimeter-Wave Gyrotron Using Metal PBG RF Cavity

4.1 Introduction

In the preceding chapter, the gyrotron's beam-wave interaction mechanism has been investigated using commercially available 3D electromagnetic PIC code "CST Particle Studio." The PIC simulation results have also been validated through the experimental published results and Multimode analysis of the gyrotron employing a three-section cavity as its RF interaction circuit. Magnetic tuning and thermal tuning have been used to obtain the tuneable bandwidth of the gyrotron.

The fabrication of millimeter-wave, sub-millimeter, and THz wave devices is a major problem because of their tiny dimensions and higher heat load per unit area of the RF structure. These problems can be reduced by designing the circuit to operate at higher-order modes, leading to mode competition problems [1]. As a result, the tuneable bandwidth of conventional gyrotrons is limited. Therefore, promising structures like photonic bandgap (PBG) structures are used to reduce the mode competition problem and enhance the tuneable bandwidth. These structures have a significantly large transverse dimension that reduces fabrication's complexity at a higher frequency [121] – [122]. Sirigiri *et al.* have demonstrated a PBG cavity-based gyrotron at 140 GHz that produced ~25 kW in the operating TE_{04} –like mode [121]. Nanni *et al.* have experimentally tested a PBG waveguide-based gyro-TWT operating in TE_{03}–like mode at 250 GHz with –3 dB bandwidth ~4.5 GHz for pulsed DNP/NMR spectrometer [123].

In the present chapter, the dispersion relation of the 2D PBG structure for triangular lattice has been presented. The PBG structure is a combination of macroscopic rods that can contain dielectric rods, metal rods, or a combination of both. The triangular lattice of the PBG structure is chosen over the square lattice due to the azimuthal symmetry, which exhibits to realize a cavity analogous to the conventional cavity. The dispersion relation has been calculated for transverse electric (TE) mode,

which provides the passband and stopband to examine the wave propagation of TE mode. The global band gap has been observed to design the PBG cavity. The present chapter's main objective is to design a PBG cavity for gyrotron oscillator to operate in $TE_{7,2}$ mode at 260 GHz. A detailed design procedure of the PBG cavity has been demonstrated and further described the designed PBG cavity's electromagnetic behavior in terms of field distribution, resonant frequency, and quality factors. A mode map has also been generated to examine all possible TE modes in the stopband. For simulations, a commercially available 3D electromagnetic code, CST Microwave Studio, is used. The scattering parameters of the PBG cavity is also determined to confirm the single-mode existence. In addition, the resonant frequency and quality factor of finite modes in metal PBG cavity are compared with those in a conventional cylindrical cavity, including other possible nearby modes. The PBG cavity design aims to achieve the mode selective operation for incorporation into the gyrotron as its RF interaction structure.

In the present chapter, the triangular lattice's dispersion characteristic of a 2D metal PBG structure has been presented. To observe TE modes' propagation, the dispersion relation has been calculated to examine the stopband and passband of the PBG structure. The mode analysis has been performed to obtain all possible modes that fall in the stopband. The design and mode analysis of the metal PBG cavity has been described in section 4.2. Section 4.3 deals with time-domain and Eigenmode analyses of the PBG cavity. The quality factors of PBG structures have been calculated in section 4.4. Further, modeling and beam-wave interaction study of 260 GHz PBG gyrotron have been discussed in section 4.5. The tuneability of PGB gyrotron operating in $TE_{7,2,q}$ –like mode is studied in section 4.6. In section 4.7, the PBG cavity's thermal and structural analyses are discussed, and the conclusion is drawn in section 4.8.

4.2 Design Methodology of the PBG Cavity

4.2.1 Dispersion Relation and Global Band Diagram

A regular triangular type PBG lattice is chosen due to its better azimuthal symmetry to realize gyrotron's interaction cavity. The periodic structure [Figure 4.1(a)] and its irreducible Brillouin zone [Figure 4.1(b)], in which Γ, X, and M are the symmetry points of reciprocal PBG structure. The conventional FDTD method is based on an explicit type Finite-Difference-Time-Domain algorithm that must satisfied Courant–Friedrich–Levy (CFL) condition. Therefore, for stability, the maximum step size is limited and must be less than a certain cell size in the computational domain that increases the simulation time. The Alternate Direction Implicit (ADI) method is known as the implicit-type Finite-Difference-Time-Domain algorithm, which has the advantage of ensuring a more efficient formulation and calculation than other implicit methods in the case of multi-dimensional problems [124]. The RF field is measured by probing at certain specified locations in the cell and at every time steps. By taking the Fourier transform, the spectrum of the field is calculated. The distributed power is measured by multiplying the RF field to its conjugate at every time steps. Then the peaks of distributed power were calculated to correspond to Eigen frequencies of the spectrum along the path Γ-X, X-M, and M-Γ of the Brillouin zone. As a result, the peaks' phase coincides with the dispersion diagram at the same location of the unit cell as shown in Figure 4.2 (a) and 2 (b) with the symbol ∇. Through the dispersion of PBG structures, its global bands [Figure 4.3] are obtained by varying the ratio of rod radius '*r*' to lattice constant '*a*'.

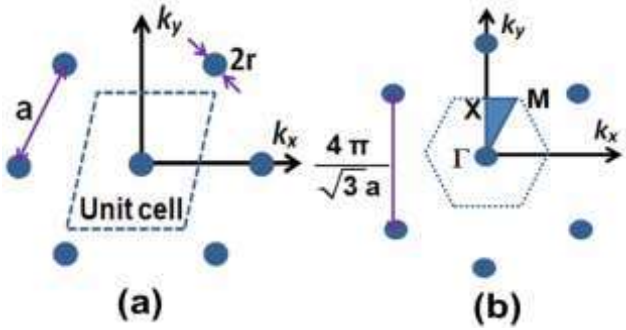

Figure 4.1 Metal PBG structures (a) unit cell in the triangular lattice (b) reciprocal lattice and Brillouin's zone (shaded area).

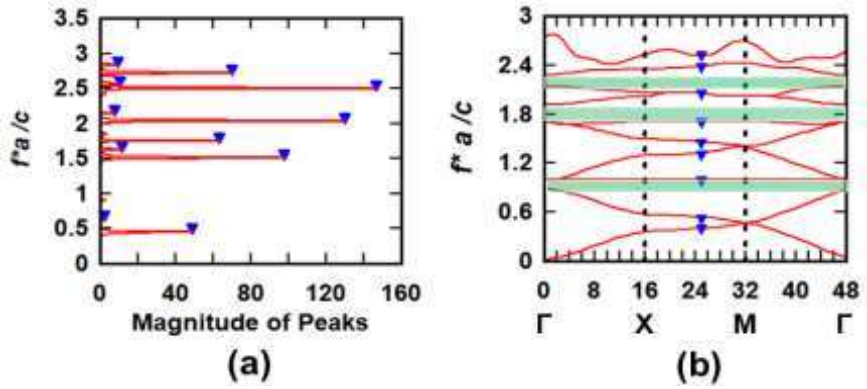

Figure 4.2 (a) Plot of normalized frequency verses peaks at certain location in the unit cell, (b) dispersion curve at r/a = 0.40.

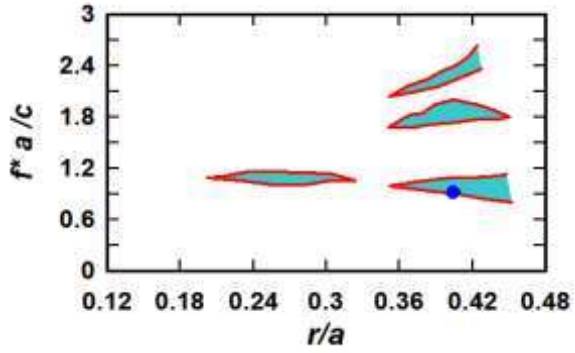

Figure 4.3 Global band-gap of the PBG cavity, where ● denotes the operating point.

4.2.2 Mode Analysis

A defect (cavity) is created at the center of the PBG structure to realize the gyrotron's RF interaction circuit. For the confinement of the desired mode within the defect, the operating point (black dot) should lie in the bandgap as shown in Figure 4.3 and other nearby competing modes should lie in the passband. The radius of the defect

in the PBG structure is approximated at par with the radius of the conventional cavity such that the desired operating mode is confined within the defect and other modes spread out of the defect. To achieve the high beam-wave interaction efficiency in gyrotron its operating mode must be pure. This is achieved by using the PBG cavity, which is realized by removing a certain number of rods from the center of the regular structure [125]. The radius of the cavity is to confine the operating mode at the operating frequency '*f*' is given by,

$$R_C = c\,\chi'_{mn} / 2\pi f \tag{4.1}$$

where x'_{mn} is the n^{th} zero roots of the m^{th}-order Bessel function $J'_m(x)$. The effective radius (R_e) of the PBG cavity after removing nineteen rods from the 2D triangular lattice is given by [125],

$$R_e = \sqrt{7}a - r \tag{4.2}$$

where, '*r*' and '*a*' are rod radius and lattice constant, respectively. By using (4.1) and (4.2), the normalized resonant frequency of the cavity operating in $TE_{m,n}$ mode is obtained as,

$$f_r a / c = x'_{mn} \Big/ 2\pi\left(\sqrt{7} - r/a\right) \tag{4.3}$$

where 'f_r' and '*c*' are the resonant frequency of the cavity and the velocity of light in free space, respectively, and '*r/a*' is the ratio of rod radius to lattice constant. Using (4.3), the possible modes confined in the defect of the PBG structure are plotted (Figure 4.4). It is observed that the mode competition is greatly reduced because the desired mode falls within the forbidden band. The modes that lie in the lower order bandgap have better coupling than modes that lie in the upper band gaps.

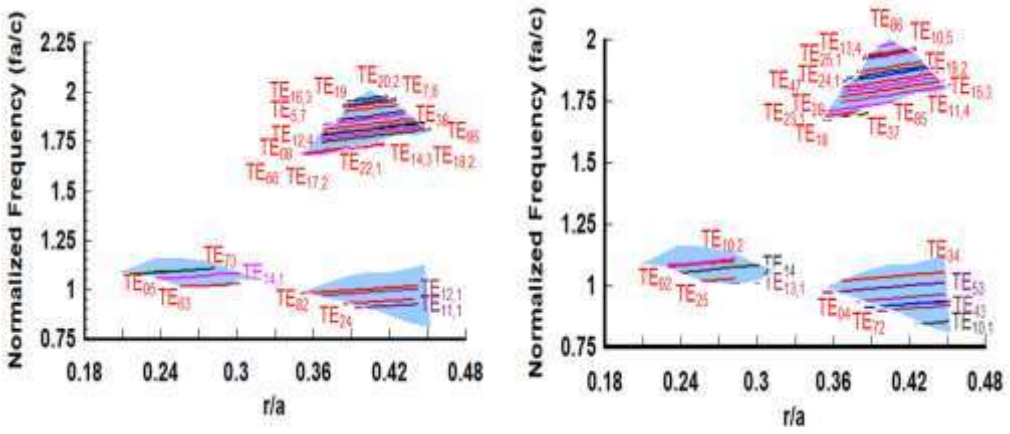

Figure 4.4 The relation between *r/a* and *fa/c* of different modes those confines in the defect after removing nineteen rods and shaded regions are the global bandgap.

4.2.3 PBG Cavity Design

In the present work, $TE_{7,\ 2}$ –like mode is chosen to study PBG gyrotron's tuneability over the conventional gyrotron [64] for DNP/NMR application. The rod radius and lattice constant of the PBG cavity are chosen in such a way that the desired mode at the specified frequency lies in the stopband and other nearby modes laid in the passband. To realize the PBG cavity as an RF interaction circuit, nineteen rods are removed from the center of the regular triangular lattice that gives the cavity radius as ~ 2.37 mm at 260 GHz. The structural parameters including the periodicity '*a*' and rod radius '*r*' of the PBG cavity are calculated as ~1.06 mm and ~0.40 mm, respectively. The cavity is modeled by using OFHC-Cu in the CST Microwave Studio with reduced conductivity $\sigma = \sigma_{Cu}/2 = 2.9 \times 10^7$ S /m. In the present study, the PBG cavity comprises a triangular lattice of metal rods used as an RF circuit in place of a straight section of conventional gyrotron. These rods are placed in parallel to the axis of the gyrotron. Two end plats with holes are also used to support the metal rods. The model of the PBG cavity is shown in Figure 4.5 (a).

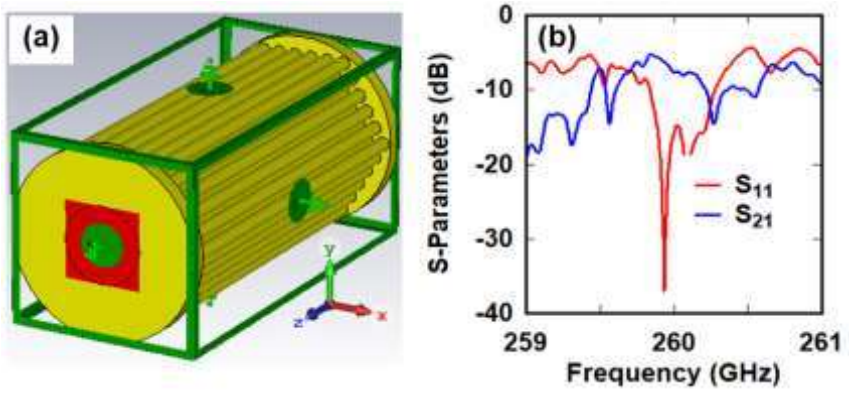

Figure 4.5 (a) Model of PBG cavity (b) S-Parameters of $TE_{7,2}$ –like mode.

4.3 Cold Analysis of the PBG Cavity

The PBG cavity is designed and simulated using "CST Microwave Studio." The Time Domain Solver and Eigenmode Solver are operated to observe the PBG cavity's transient and electromagnetic behaviors, respectively. The design parameters of the PBG cavity are listed in Table – 4.1.

4.3.1 Time Domain Analysis

The modeled cavity was excited with a Gaussian pulse to study its mode confinement property and losses in an electron beam's absence (cold analysis). The Perfectly Match Layer (PML) boundary is chosen for the present simulation and set the tangential component of the electric field (E–field) as zero, *i.e.* $E_t = 0$ [Figure 4.5 (a)] and the surrounding space is a vacuum in the radial direction, which is used as an absorbing layer to minimize the reflection. This boundary condition automatically adds extra space between the structure and the applied open boundary, which is called a bounding box with six faces. The propagation behavior of the PBG cavity is studied through the Scattering parameters (*S*–parameters) [Figure 4.5 (b)], which shows that S_{21} of – 6.26 dB and S_{11} of –36.80 dB for $TE_{7,2}$ –like mode at 259.96 GHz.

4.3.2 Eigenmode Analysis

In the present study, the Eigenmode Solver is used to examine all possible modes that lie in the frequency range of 255 GHz – 265 GHz. To avoid the TM modes in the simulation, the magnetic wall ($H_t = 0$) is used at both the transverse plane of the PBG cavity, as shown in Figure 4.6. The magnetic wall works well for the TE mode confinement without longitudinal variation in the electric field's amplitude. Only a short longitudinal length (quarter wavelength) of the PBG cavity is used in simulations that help to simulate the structure within a reasonable time with the limited available memory of resources. However, the gyrotron is operated in a TE_{721} –like mode in which the axial length of the resonator is approximately ~ 20 times the operating wavelength. The PBG resonator's mode density can be compared with an analogous cylindrical resonator by examining their Q-factor and resonance frequency. The transverse dimension of the cylindrical resonator is about 4.74 mm, while the transverse dimension of the PBG resonator is about 11.8 mm, as shown in Figure 4.7 (a) and 4.7 (b), respectively. It is assumed that no longitudinal variation occurs in the electric field of $TE_{m,n,1}$ mode. In a cylindrical resonator, the ohmic loss is due to the finite conductivity of the resonant wall, while in the PBG resonator the ohmic loss is due to the finite conductivity of metal rods. Therefore, a final boundary wall is included in the modeling of PBG structures. Practically, the PBG resonator does not have an outer wall; therefore, the Q factor of the PBG resonator presented here is expected to be slightly higher.

The desired $TE_{7,2}$ –like mode is confined within the defect (cavity) in the PBG cavity [Figure 4.7 (b)], which is very much analogous to the conventional $TE_{7,2}$ mode [Figure 4.7 (a)]. However, there is an intense leakage of E-field of all spurious competing modes, including TE4,3 –like and TE2,4 –like modes in the PBG cavity's transverse direction. Due to the strong leakage of competing modes, the ohmic quality factor

Table 4.1 Resonating frequency and quality factor of RF cavities

Mode	Cylindrical Cavity		PBG Cavity (like mode)	
	Res. Freq. (GHz)	Ohmic Q	Res. Freq. (GHz)	Ohmic Q
$TE_{4,3}$	255.03	13800	258.03	7800
$TE_{11,1}$	257.87	4190	254.52	4840
$TE_{7,2}$	260.05	11550	260.31	10552
$TE_{2,4}$	264.77	16720	264.59	4459
TE_{04}	267.90	16400	264.42	7480

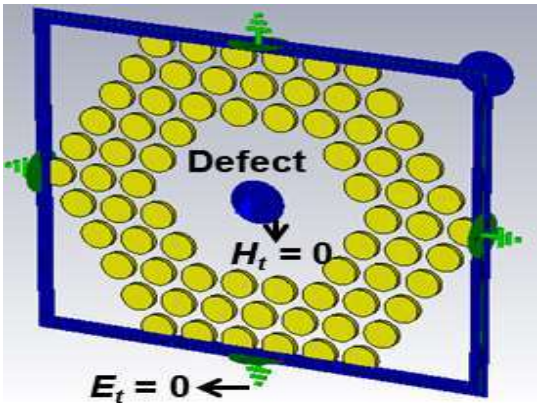

Figure 4.6 Boundary condition around the PBG cavity in the Eigenmode analysis.

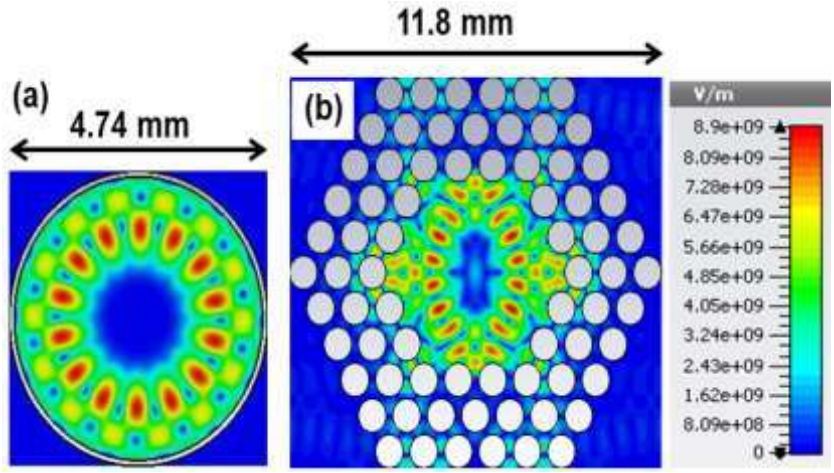

Figure 4.7 (a) E- field pattern of the $TE_{7,2}$ mode in the conventional cavity and (b) $TE_{7,2}$ –like mode in the PBG cavity.

(Q) of competing modes is decreased as compared to the cylindrical resonator, as listed in Table – 4.1. However, the desired $TE_{7,2}$ –like mode has a higher ohmic Q factor of 10,552, as expected in the PBG resonator.

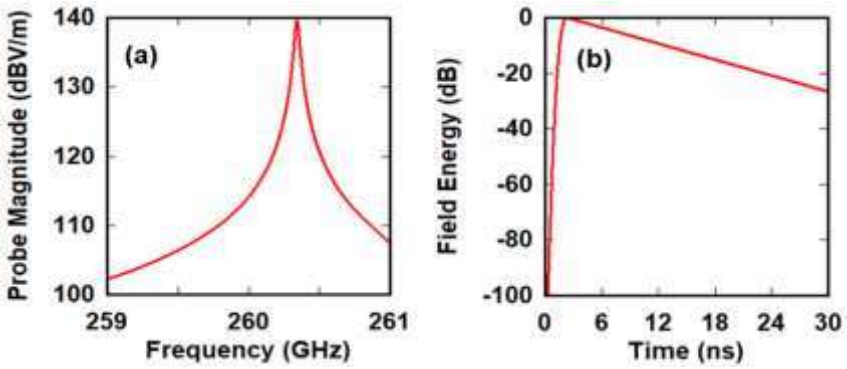

Figure 4.8 (a) Spectrum of the probed E-field, and (b) Stored energy decay.

4.4 Calculatiion of Quality Factor

The Q-factors provide the estimation of various losses in the structures, as explained in Chapter – 2. To estimate the ohmic Q-factor (Q_{ohm}) and diffractive Q-factor (Q_d), the cavity is simulated in "CST Microwave Studio" with the relevant boundary conditions. The Q_{ohm} is associated with the loss due to the metal surface's finite conductivity. The Q_d is associated with the loss due to the EM leakage through the PBG cavity. The overall Q factor is calculated by using (2.60).

The Q_d is determined by exciting the PBG cavity with a discrete current source. To determine the 'Q_d' for TE polarization, symmetry planes XZ and YZ with $E_t = 0$ along with a magnetic boundary condition, $H_t = 0$, in XY plane are defined along with the open boundary condition in all directions [126]. The E-field distribution is recorded by inserting a probe in the cavity, where the maximum field is expected. The probed field is then passed through an Auto-Regressive (AR) filter to eliminate the truncation errors. The AR filtered probe spectrum [Figure 4.8 (a)] can be used to directly calculate the 'Q_d' by using the ratio of the resonant peak frequency (f_r) to –3 dB points from the peak with good accuracy. Another method is to calculate the 'Q_d' from the energy decay [Figure 4.8 (b)] in the PBG cavity, which is given by,

$$Q_d = \frac{2\pi f_r}{0.693}\Delta t \tag{4.4}$$

where, Δt is a time interval, which is calculated by considering –3dB energy decay in the linear decay section of the curve. In the present design, the 'Q_d' is obtained as ~7400 for the desired operating $TE_{7,2,1}$ –like mode at ~260.31 GHz.

To estimate the ohmic Q factor, the Eigenmode Solver of "CST Microwave Studio" is used, as described in the previous section 4.3.2. For calculating the Q_{ohm}, the conductivity of the copper material has been considered as, σ = 2.9 ×10^7 S /m, permeability = 1, density = 8978 kg /m^3, and the thermal conductivity = 390 W /K–m). In the Eigenmode simulation, the smooth surface is considered, *i.e.*, the surface roughness is assumed to be zero. The variation in the temperature of the rods is also not taken into account, while the boundary temperature is considered as isothermal. The cooling of the rods is not considered. The calculated Q_{ohm} of the operating $TE_{7,2}$ –like mode and other competing modes are listed in Table – 4.1.

4.5 Design and PIC Simulation of PBG Gyrotron

4.5.1 Modeling of PBG Gyrotron

The present gyrotron mainly consists of three sections [Figure 4.9 (a)], including a down taper, a metal PBG cavity as an RF interaction circuit, and an uptaper. The mode analysis and cold characterization of the PBG cavity are discussed in section 4.3, showing that the PBG cavity with the mode selective / frequency selective property behaves like a conventional cavity. To maximize the beam-wave interaction, the RF field's amplitude must be maximum in the middle of the interaction cavity. The RF field profile [Figure 4.9 (b)] is obtained with respect to the axial length of the cavity using (2.86) - (2.87) with the corresponding diffractive Q-factor (Q_d). Using both structural and electrical parameters given in Table – 4.2, the present PBG gyrotron

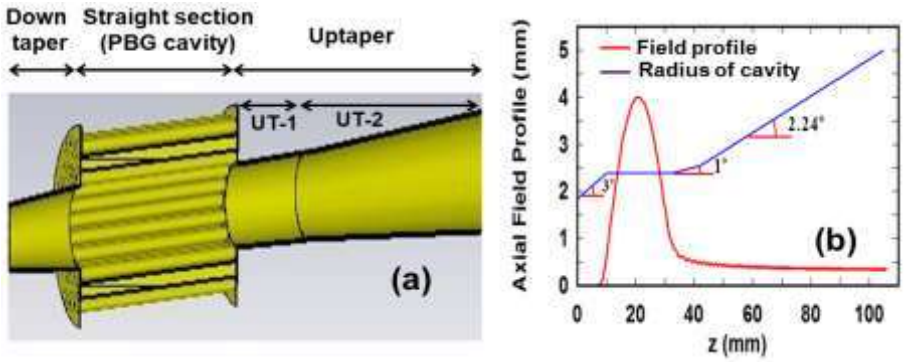

Figure 4.9 (a) Model of PBG gyrotron (b) normalized field profile with the radius of the gyrotron cavity.

[Figure 4.9 (a)] is modeled in "CST Particle Studio" along with the particle emitter. In order to select the appropriate mesh setting in the PIC simulation, the mode convergence analysis of the PBG cavity has been performed using the Eigenmode solver. The confined frequency in the PBG cavity begins to converge at 3 cells per wavelength (fraction of 6 cells near the model) and 6 cells per wavelength (fraction of 3 cells near the model), as shown in Figure 4.10. The same confined frequency (~260.31GHz) is found at 3 cells per wavelength (fraction of 6 cells near the model) and 6 cells per wavelength (fraction of 3 cells near the model). Due to the system's computational problem at higher mesh cells, 3 cells per wavelength (6 cells near the model) with total mesh cells 1, 40, 57,200 have been chosen in the PIC simulation. In the present design, the length of the cavity and the angle of tapers are optimized with the field profile's help. Further, the field inside the PBG cavity, i.e. far from the boundary of rods towards the center of the defect, is symmetric, and which is very similar to the field profile in a conventional cavity. This symmetric field in the PBG cavity can couple to the hollow annular electron beam [127] similar to the conventional gyrotron. The radius of the electron beam (R_b) is chosen such that the coupling between the beam and RF field is maximum. The RF field is polarized either co-rotating or counter-rotating with respect to gyrating electrons. The coupling coefficient is

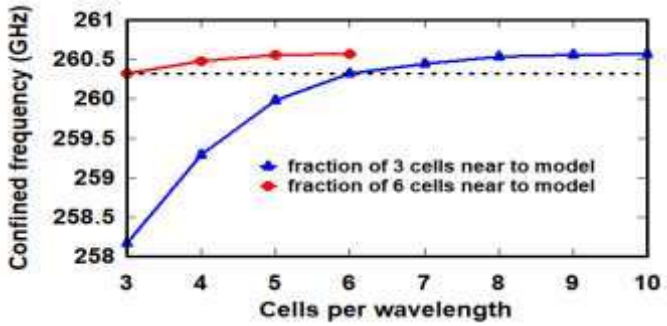

Figure 4.10 Confined frequencies in the PBG cavity with respective cells per wavelength.

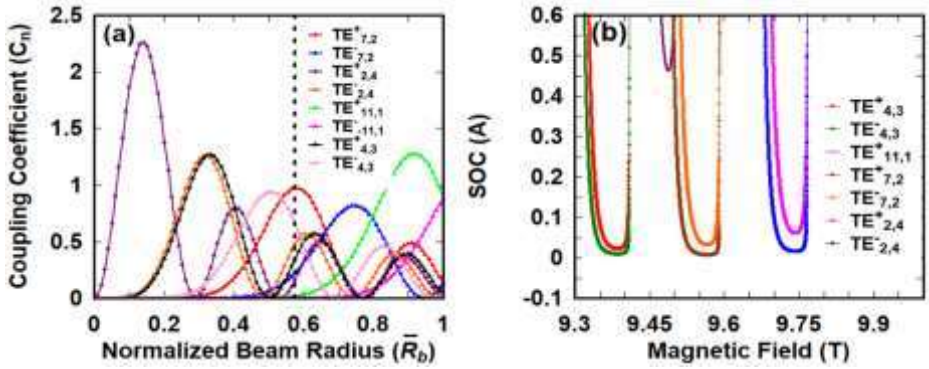

Figure 4.11 (a) Relation between coupling coefficient and normalized beam radius (b) SOC of $TE_{7,2,1}$ mode and its nearby competing modes.

calculated by using (2.81). It is observed from Figure 4.11 (a), the coupling coefficients of counter-rotating $TE^{-}_{7,2}$, $TE^{-}_{11,1}$ and co-rotating $TE^{+}_{4,3}$, $TE^{+}_{11,1}$, $TE^{+}_{2,4}$ modes are minimum at the normalized beam radius of ~0.58 for s = 1, but the counter-rotating $TE^{-}_{2,4}$ and $TE^{-}_{4,3}$ modes are closely competing with the desired co-rotating $TE^{+}_{7,2}$ mode. As a result, a co-rotating (right-handed) $TE_{7,2}$ mode and a counter-rotating (left-handed) $TE_{2,4}$ mode are excited. The gyrating electron beam's guiding center radius is calculated as ~1.374 mm with an outer radius of ~1.414 mm and an inner radius of ~1.334 mm. The start oscillation current (SOC) [Figure 4.11 (b)] of the desired $TE_{7,2}$ mode and its nearby competing modes including $TE_{4,3}$ and $TE_{2,4}$ is minimum at the magnetic field of 9.56T and 9.40T, and 9.75T, respectively. The excitation of spurious competing modes $TE_{4,3}$ and $TE_{2,4}$ are at a span of ~0.35 T and the desired $TE_{7,2}$ –like mode is excited within this span, therefore the magnetic tuning of the desired mode is possible.

Table: 4.2 Design Parameters of PBG Gyrotron

Structural Parameters	Down taper	Length (mm)	10
		Angle	3°
	RF section (PBG Cavity)	Length (mm)	22
		r (mm)	0.40
		a (mm)	1.06
	UP Taper (1)	Length (mm)	10
		Angle	1°
	UP Taper (2)	Length (mm)	63
		Angle	2.24°
Beam Parameters	Voltage	15.5 kV	
	Current	140 mA	
	Frequency	260.317 GHz – 260.85 GHz	
	Pitch factor	1.7	
	Beam radius (mm)	1.374	
	Beam width (mm)	0.08	
	Velocity spread	~ 2%	
	Magnetic field	9.53 T – 9.75 T	
	Output Power	≥ 1.5 W	

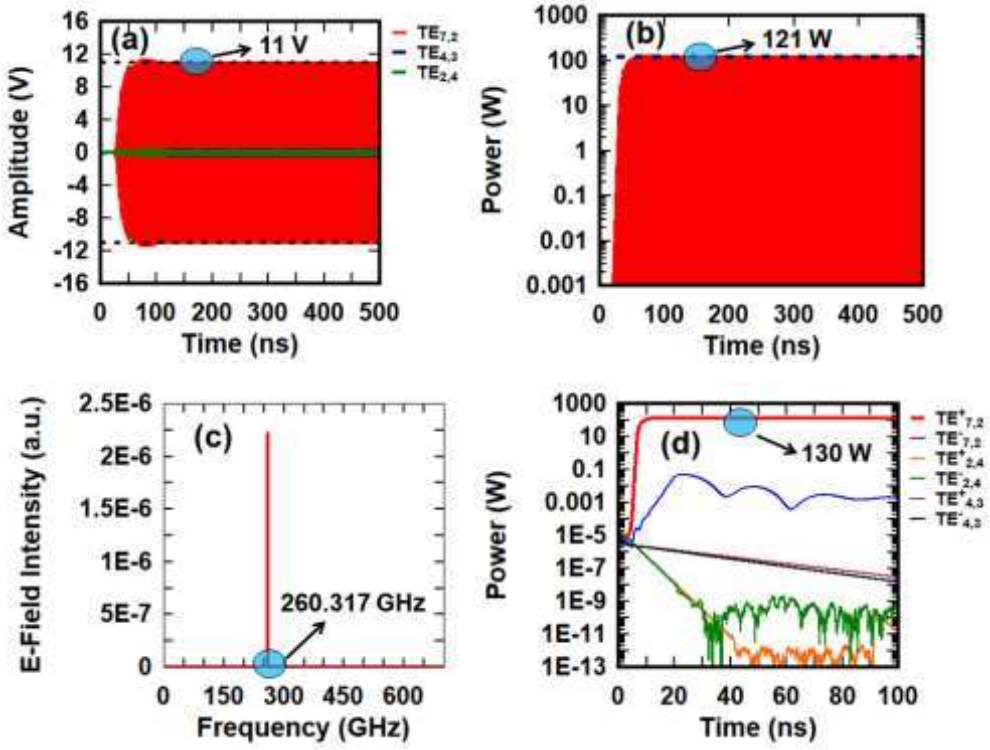

Figure 4.12 (a) Amplitudes of port signals (b) power in $TE_{7,2,1}$-like mode (c) frequency spectrum of the port signal of $TE_{7,2,1}$ –like mode (d) output power through Multimode time-dependent calculation. The beam parameters 15.5kV, 140mA, and α= 1.7 with 2% velocity spread are considered in the PIC simulation and Multimode simulation.

4.5.2 PIC Simulation of PBG Gyrotron

The modelling of the gyrotron in PIC simulation environment and the beam-wave interaction process have already been narrated in Chapter – 3. In the present hot simulation, a total of 144 emission points are considered in the cathode surface with the beam voltage 15.5 kV, and beam current 140 mA. Initially, the Larmor radii and energy of all beamlets remain the same as ~1.374 mm and ~15.5 keV, respectively. At the output side, the Larmor radii and energy of all beamlets are modulated due to the perturbation of the RF wave. The change in Larmor radii and cyclotron frequency of electrons leads to the phase bunching of electrons. Once the bunching of electrons takes place, some electrons begin to transfer their kinetic energy to the RF field, resulting in an increase in the RF signal at the output port. The temporal growth of the developed signal in $TE_{7,2,1}$ –like mode and other competing modes is shown in Figure 4.12 (a). The RF signal amplitude of $TE_{7,2,1}$ – like mode is observed as ~11 V. The CW RF output power [Figure 4.12 (b)] of ~121W in $TE_{7,2,1}$ –like mode is obtained with the beam parameters, 15.5 kV, 140 mA, $\alpha = 1.7$ and velocity spread 2 %. The observed output power in $TE_{7,2,1}$ –like mode is maximum as compared to other competing modes. This is achieved by the frequency selective property of the PBG structures that provides a heavy attenuation to spurious $TE_{4,3}$ and $TE_{2,4}$ modes and pushes them to propagate in the PBG circuit's transverse direction. Simultaneously, the PBG circuit is confining the desired $TE_{7,2}$ –like mode in its defect with a high-quality factor, hence maximum output power is achieved in the desired mode. The spectrum [Figure 4.12 (c)] is obtained by taking the Fourier Transform of the developed signal at the output port of the PBG gyrotron that confirms the device's operating frequency at ~260.317 GHz in $TE_{7,2,1}$ –like mode. Further, the present 3D PIC simulation and mode competition studies of PBG gyrotron are validated using a time-dependent self-consistent nonlinear theory [91]. The

electric field patterns [Fig. 4.7 (a)] of confined modes in both conventional and PBG cavities are very close to each other, the only difference between conventional cavity and PBG cavity are resonating frequency and quality factor: the former 260.05 GHz with quality factor 11550 and later 260.31 GHz with quality factor 10552. It is a good approach to treat a PBG cavity as a conventional cavity with mode selectivity for the Multimode simulation. In the present nonlinear Multimode calculation of PBG gyrotron, both co-rotating (+) and counter-rotating (–) components of the desired and competing modes are considered. Figure 4.12 (d) predicts a maximum power of ~130 W in $TE^{+}_{7,2}$–like mode and negligible power is found in competing modes including $TE^{+}_{4,3}$, $TE^{+}_{2,4}$, $TE^{-}_{7,2}$, $TE^{-}_{4,3}$ and $TE^{-}_{2,4}$–like modes. It shows that the competing modes are well suppressed as needed for single-mode operation of the device.

4.6 Tuneability of PBG Gyrotron

In the present chapter, magnetic tuning is performed to achieve the tuneable bandwidth of the gyrotron. The procedure of the magnetic tuning scheme has been described in Chapter – 3. The resonant frequency and the present PBG gyrotron's output power are calculated with respect to the magnetic field at a constant beam voltage. The axial mode number (q) of the confined $TE_{7,2,q}$ –like mode is varied from 1 to 4 by varying the magnetic field. In the magnetic tuning, the resonant frequency of the electromagnetic mode is a function of the magnetic field. The PBG cavity allows multiple radiation maxima along its axial length. The $TE_{m,n,1}$ mode is expected to excite but in addition to that, a series of $TE_{m,n,q}$ modes are also excited, where, 'q' is an integer greater than one. The range of tuning frequency is generally the difference between the minimum and maximum resonating frequencies of $TE_{m,n,q}$ modes. The higher-order

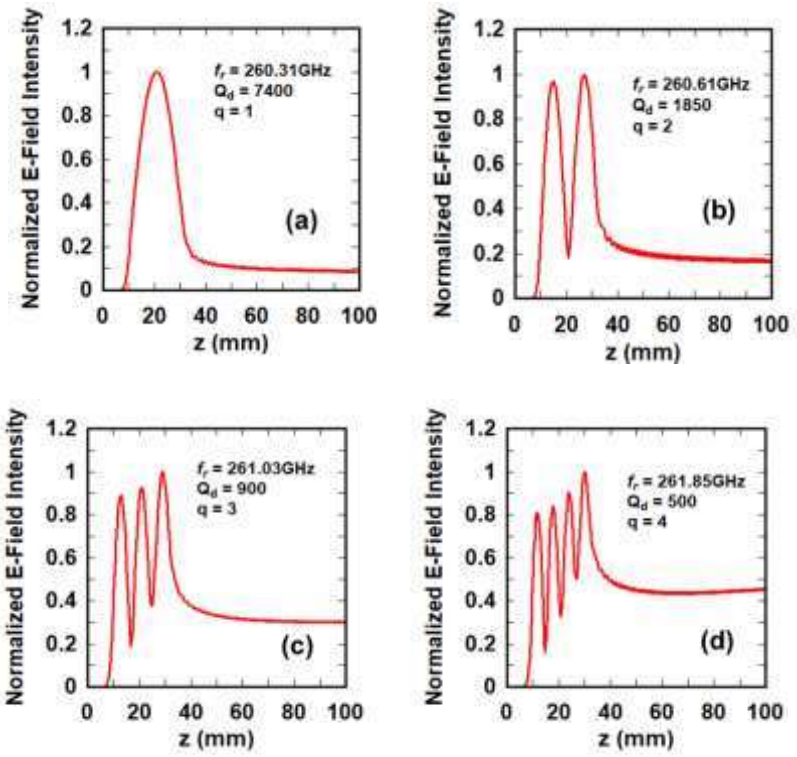

Figure 4.13 Axial electric field variation inside the cavity in absence of electron beam, for (a) q = 1 (b) q = 2 (c) q = 3 and (d) q = 4.

axial modes have a higher resonating frequency, excited at higher magnetic field value and beyond where the $TE_{m,n,1}$ mode is excited [99]. This is evident in the cold field profile [Figure 4.13 (a)–(d)] for various axial mode numbers, q = 1 to 4 in the present case. In the present 3D simulation, the CW output power and resonant frequency [Figure 4.14 (a)] of $TE_{7,2,q}$ –like PBG mode are calculated by varying the magnetic field. These results are validated by using a Multimode nonlinear code and found that they are in close agreement. To calculate the tuneable bandwidth, the CW output power is observed with respect to the resonant frequency [Figure 4.14 (b)] by varying the axial index (q = 1, 2, 3, and 4) of the desired $TE_{7,2,q}$ –like mode. The lowest resonating frequency is observed as ~260.317 GHz for q = 1 at ~9.53T with a CW output of ~121W and the higher resonating frequency is ~261.85 GHz for q = 4 at ~9.75T with more than ~1.5W. Therefore, a continuous broad frequency tuning of more than 1.5 GHz is obtained in the present PBG gyrotron. The results obtained from PIC

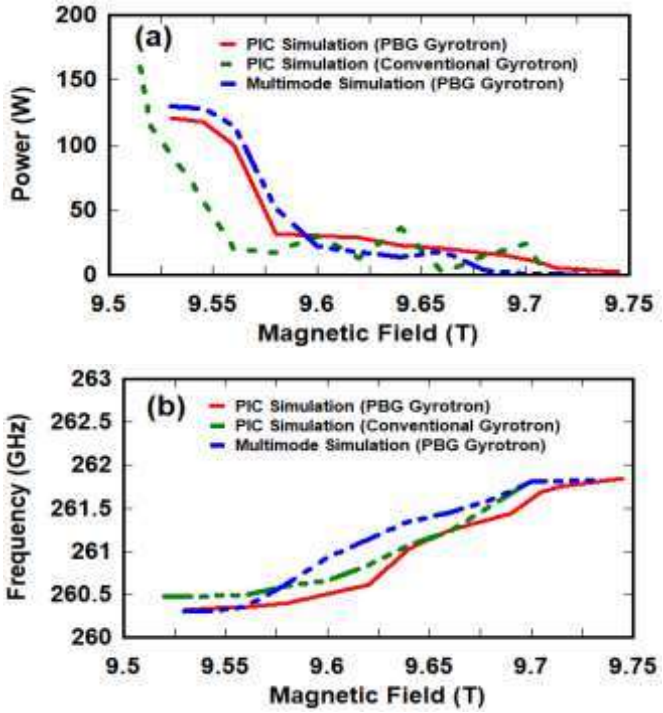

Figure 4.14 Comparison of (a) power and (b) frequency / bandwidth of PBG gyrotron and conventional gyrotron [95] over magnetic field using PIC simulation and Multimode code (PBG gyrotron) for V_0 = 15.5 keV, I_0 = 140 mA, and α = 1.7 with 2 % velocity spread.

simulation of the present PBG gyrotron have been compared with the results of the conventional gyrotron studied in Chapter – 3 operating at the same frequency [Figs. 4.14 (a) and 4.14 (b)]. It is observed that the tuneable bandwidth (~1.5 GHz) of PBG gyrotron is higher than the tuneable bandwidth (~1.3 GHz) of conventional gyrotron [95] as shown in Figure 4.14 (b).

4.7 Thermal and Structural Analyses of PBG Cavity

The present gyrotron's PBG cavity is modeled using a smooth annealed copper having the reduced conductivity, $\sigma = 2.9 \times 10^7$ S/m, and other properties of annealed copper are kept as same as given in Table – 3.1 of Chapter – 3. Some of the RF power generated in the PBG cavity is lost due to the metal rods' finite electrical conductivity. The temperature distribution profile [Figure 4.15 (a)] in the PBG cavity is studied for q = 1 of $TE_{7,2,q}$ –like mode. This is obtained by importing the loss profile of the PBG cavity's metal rods from the cold analysis to the transient thermal solver. The

Table 4.3: Deformation of the PBG Cavity

q	Power(W)	Deformation of the cavity					
		Inner layer		Middle layer		Outer layer	
		Temp. (K)	Δr (μm)	Temp. (K)	Δr (μm)	Temp. (K)	Δr (μm)
1	121	314.04	0.128	310.31	0.103	310.17	0.102
2	25.4	310.01	0.101	307.85	0.086	307.33	0.082
3	20.5	306.10	0.074	304.21	0.061	303.88	0.059
4	10.2	302	0.046	300.57	0.036	300.54	0.036

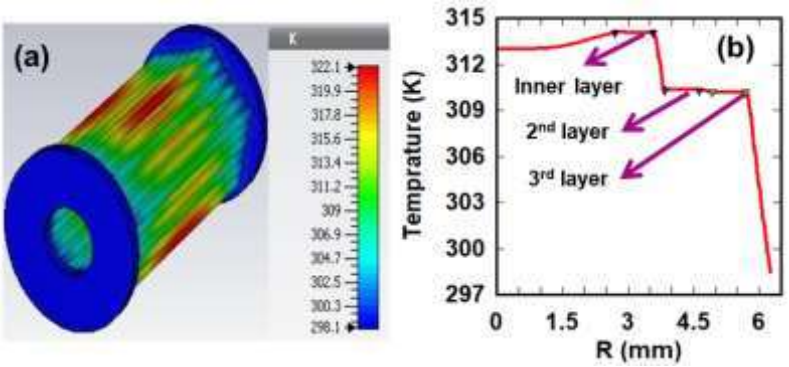

Figure 4.15 Temperature (a) profile in the PBG cavity and (b) distribution in the radial direction.

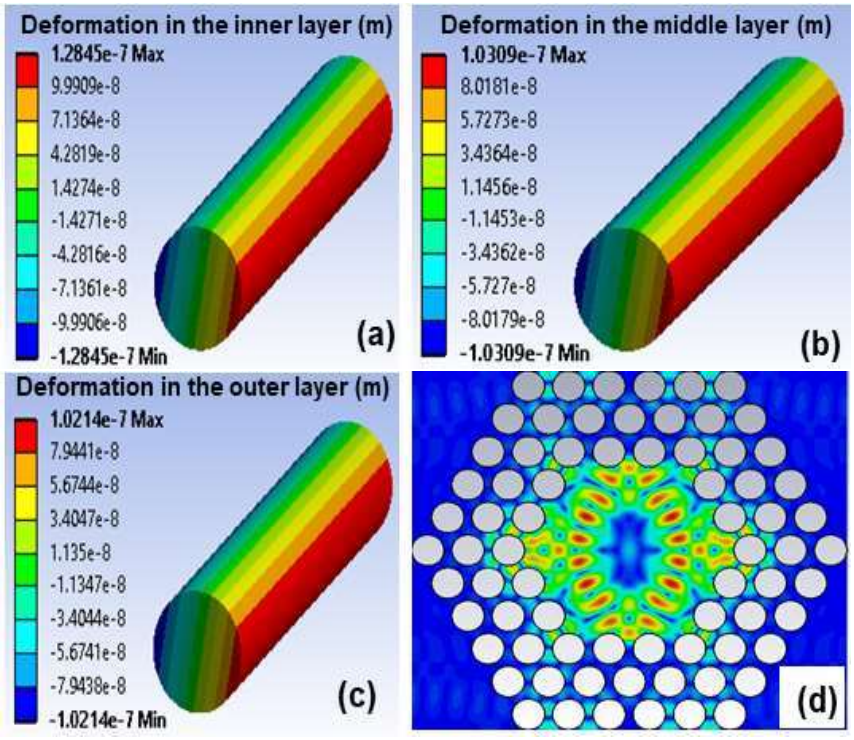

Figure 4.16 Deformation of rods in the PBG cavity (a) inner layer (b) middle layer (c) outer layer (d) E-field pattern resonating at 260.324 GHz.

starting temperature over the radial distance of the PBG cavity including its inner, middle, and outer layers [Figure 4.15 (b)] is observed as ~314.04K, ~310.31K, and ~310.17K, respectively. The temperature difference in various layers of the PBG structures can deform the shape of the metal rods. The excitation of the RF signal at a particular frequency depends upon '*a*' and '*r*' of the rods. The structural deformation of the PBG cavity might change the frequency of the mode excited. To observe structural deformation's effect on the resonant frequency of the cavity, the structural analysis is done by using a commercially available FEM-based code, ANSYS [113]. For thermo-mechanical simulation, the PBG rods are modeled by using isotropic, and elastic OFHC-Cu material with both ends of rods are fixed in ANSYS. The standard earth gravity (9.8 m /sec^2) is considered in the simulation. The rod is free to expand in the radial direction and fine meshing type is used in the simulation. The temperature is calculated using the thermal transient solver of "CST Mphysics Studio", which is used as a thermal load to obtain the deformation of rods in the Static Structural Solver of ANSYS. It is observed that the deformation in the radii of rods at the inner, middle, and outer layers as ~0.128 μm [Figure 4.16 (a)], ~0.103 μm [Figure 4.16 (b)], and ~0.102 μm [Figure 4.16 (c)], respectively, for the RF output power of ~121 W in $TE_{7,2,q}$-like mode with q = 1. The resonance of $TE_{7,2,1}$ –like mode [Figure 4.16 (d)] in the PBG cavity using deformed rods is shifted by ~7 MHz. A similar exercise was repeated to observe the deformation in metal rods for other axial mode numbers of $TE_{7,2,q}$ –like mode including q = 2, 3, and 4, as listed in Table – 4.3.

4.8. Conclusion

In the present chapter, the metal PBG cavity's mode selectivity has been investigated by analyzing its electromagnetic behavior. The dispersion characteristics of

the 2D metal PBG structure for TE mode have been studied by using the ADI-FDTD method that is less cumbersome and easier to implement. The global band gap has been calculated by using the dispersion relation at the various ratio of rod radius to lattice constant. Mode analysis has been performed to obtain all possible modes confined in the defect of the PBG cavity. The propagation characteristics and resonating frequency have been calculated by using the Time Domain Solver and Eigenmode Solver of "CST Microwave Studio", respectively. The present study of metal PBG structures has laid the pavement to understand their electromagnetic behavior and is motivated to use it as an RF interaction circuit in gyrotron devices.

In the present chapter, a millimeter-wave CW gyrotron using a metal PBG cavity as its RF circuit has been designed and studied for its beam-wave interaction behavior. The PBG gyrotron has been designed and simulated in the "CST Particle Studio" to observe the transient characteristics. Magnetic tuning has been performed to obtain tuneable bandwidth of the PBG gyrotron in which a series of axial modes are excited in the PBG cavity. The present gyrotron's tuneability has been achieved with an RF output power of more than ~1.5 W for DNP/NMR applications. The PBG gyrotron's magnetic tuning exhibited a bandwidth of more than ~1.5 GHz as the axial mode number (q) of the desired $TE_{7,2,q}$ –like mode varied from 1 to 4. Further, the thermal effects on the present PBG gyrotron's performance were carried out by including the structural deformation in the metal rods. The resonating frequency was shifted only by ~7 MHz due to the deformation of rods. The shift was observed that it is meager and negligible as the thermal loading in the PBG cavity is very less due to its large transverse area. Therefore, it is hoped that the proposed low power PBG gyrotron can provide stable operation even in the absence of cooling rods. The stable operation of such type of source may be useful for DNP/NMR spectroscopy applications.